Indonesian Journal of Material Research
e-ISSN: 2987-1654
Vol. 3, No. 2, July 2025

Indonesian Journal of MATERIAL RESEARCH

Research Paper

Eucheuma cottonii Hydrochar: A Promising Adsorbent for Congo Red Dye

Bunga Indah Putri[1], Fitri Suryani Arsyad[1,2], Yulizah Hanifah[4], Nur Ahmad[3*]

[1] *Master Program of Materials Science, Graduate School, Universitas Sriwijaya, Palembang, 30662, Indonesia*
[2] *Department of Physics, Faculty of Mathematics and Natural Sciences, Sriwijaya University, Palembang, 30139, Indonesia*
[3] *Research Center of Inorganic Materials and Coordination Complexes, Universitas Sriwijaya, Palembang, 30662, Indonesia*
[4] *Research Center for Chemistry, National Research and Innovation Agency, Building 452 KST BJ Habibie, Tangerang Selatan, 15311, Indonesia*
[*]**Corresponding author**: nurahmadtula23@gmail.com

Abstract
This study investigates the transformation of *Eucheuma cottonii* (EC) into a highly efficient adsorbent through hydrothermal carbonization at 200°C, resulting in hydrochar (HC-200). The FT-IR analysis reveals significant structural changes, including reduced intensity of oxygenated functional groups such as carbonyl and hydroxyl, alongside increased aromaticity, contributing to enhanced hydrophobicity and structural stability. These alterations render HC-200 well-suited for adsorption applications. BET analysis highlights a marked increase in the specific surface area and mesoporosity of HC-200 compared to EC, with hysteresis loops confirming enhanced adsorption capacity. SEM imaging shows substantial morphological changes, including rougher surfaces, increased porosity, and the presence of spheroidal structures, indicative of successful carbonization and improved diffusivity. Adsorption studies underline HC-200's superior performance in anionic dye removal, with a maximum adsorption capacity 37.894 mg/g. pHpzc analysis demonstrates more acidic surface characteristics, which favor adsorption in acidic conditions. Adsorption kinetics align predominantly with the pseudo-second-order model, indicating chemisorption as the dominant mechanism. The regeneration study shows HC-200's excellent reusability, maintaining significant adsorption efficiency over seven cycles, whereas EC experiences a steep decline in performance.

Keywords
Eucheuma cottonii, Macroalgae, Hydrochar, Hydrothermal, Congo Red

Received: 8 April 2025, Accepted: 14 July 2025
https://doi.org/10.26554/ijmr.20253264

1. INTRODUCTION

Textile dyeing is one of the largest industrial polluters, accounting for 20% of wastewater production globally (Ramesh et al., 2024). In particular, the textile sector releases highly toxic and non-biodegradable dyes that seriously harm the environment, leading to a substantial amount of water pollution. Congo Red (CR) is a dye prevalently used in industry (Lesbani et al., 2025). Due to its exceptional chemical stability and resistance to natural degradation, this anionic azo dye is widely recognized (Kumar et al., 2018). It has been discovered that CR can be carcinogenic, harm human organs and the environment due to its and ability to disrupt aquatic ecosystems by impeding photosynthesis in marine plants (El Bourachdi et al., 2025). Therefore, it is essential to create and implement effective wastewater treatment techniques to remove diazo dye.

Various techniques have been developed to remove diazo dye from wastewater, such as coagulation, photodegradation, oxidation, and biological processes. They frequently struggle to adequately eliminate these dyes because of their complex molecular structure and chemical stability (Tehrani et al., 2024). Despite their benefits, these approaches have inherent drawbacks as well. These include the potential risks connected to the application of specific chemicals and the additional problem of handling generated sludge, which might raise its own set of environmental issues. Among the several available approaches, adsorption is a particularly efficient and economical technology (Ghosh et al., 2021). Its benefits include ease of use and the ability to eliminate dyes without producing any hazardous by-products (Deng et al., 2024). *Eucheuma cottonii* (EC) has surfaced as a promising raw material for hydrochar production. Plentiful and readily accessible, EC consists of polysaccharides and various organic elements that can be efficiently transformed into adsorbents with favorable characteristics (Wibiyan et al., 2023). Using this marine biomass is by sustainable development principles as it encourages waste valorization and lessens environmental impact. Hydrothermal carbonization (HTC) is a highly effective, adaptable, and environmentally friendly process that is commonly used to treat wet solid waste (de Tuesta et al., 2021), thereby addressing the pressing need for effective waste management strategies (Funke and Ziegler, 2010). HTC

produces hydrochar, the main solid by-product, which is regarded as a waste-to-char product. Its high energy density, low sulfur, functional groups that facilitate dye adsorption, chlorine concentration, and high carbon content are characteristics of natural lignite. Nevertheless, the hydrochar produced by HTC frequently has a low porosity and surface area, which restricts its use as a catalyst or adsorbent (Chen et al., 2021).

Biochar Carbon-dense substance produced from the thermal breakdown of biomass, has received notable interest as a potential adsorbent for treating wastewater. Biochar in dye adsorption can be improved further by employing advanced processing methods like HTC. It is commonly known that the thermally treated material is broken down into three different fractions during the pyrolysis process, a thermochemical reaction that takes place in an inert atmosphere and at atmospheric pressure: solid (char), gas, and liquid (condensable liquids or oils) (Bridgwater, 2012). However, it should be mentioned that a significant amount of energy is used during pyrolysis at high temperatures (over 600°C) because of the thermochemical change of organic matter (Blondeau and Jeanmart, 2012). Furthermore, the high moisture content of biomass waste products usually calls for pre-drying before high-temperature heat treatment. HTC at low temperatures using conventional or microwave heating is a feasible substitute for high-temperature thermal treatment, including pyrolysis (Hoekman et al., 2011). Depending on the feedstock's composition and the process parameters (temperature, reaction time, pressure, and solid/water ratio), hydrochars' structure, composition, and possible uses vary greatly. HTC is still only available at the laboratory or demonstration scale (under TRL) despite its scientific acknowledgment (Munir et al., 2018). Although HTC has long been used to produce fuels and explain the coalification process, its production of hydrochar has received more attention (Kruse and Dahmen, 2018).

The objective of this research is to explore the use of hydrochar sourced from EC for the adsorption of CR dye. The study centers on examining the adsorption capability, investigating the fundamental mechanisms, and determining the effectiveness of hydrochar in eliminating CR from water solutions. This study offers insights into the capabilities of adsorbents derived from EC, aiding the creation of environmentally friendly and affordable options for treating dye-polluted wastewater.

2. EXPERIMENTAL SECTION

2.1 Materials and Methods

2.1.1 Materials and Characterization

Macroalgae *Eucheuma cottonii* were sourced from the coastal waters of Maluku, Indonesia. The study utilized distilled water (H_2O), Congo Red (CR) dye, Potassium Chloride, Potassium Hydroxide, and Chloride Acid. The macroalgae were analyzed using a Shimadzu Prestige-21 FT-IR spectrophotometer, BELSORP-miniX BET surface area analyzer, and Scanning Electron Micros cope-Energy Dispersive X-Ray (SEM-EDS) type Quanta 650 and Rigaku MiniFlex600 X-Ray Diffractometer. Dye solution absorbance was measured with a UV-visible Biobase spectrophotometer UV BK-1800PC.

2.1.2 Preparation of Macroalgae *Eucheuma cottonii*

EC was first thoroughly washed to remove any residual dirt and salt, with multiple washes to ensure cleanliness. The macroalgae were then rinsed with distilled water and dried in an oven at 80°C for 5 h to eliminate moisture (Farobie et al., 2023). Once dried, the macroalgae was ground into a fine powder and sifted through a 200-mesh screen. The processed material was then characterized using FT-IR, BET and SEM-EDS techniques.

2.1.3 Preparation of Hydrochar *Eucheuma cottonii*

To begin, 2.5 g of finely ground EC macroalgae was mixed with 50 mL of distilled water. This mixture was then homogenized by stirring with a magnetic stirrer for 3 min before being transferred into a hydrothermal autoclave. The hydrothermal treatment was performed at temperatures of 200°C for 3 h. Afterward, the samples were dried in an oven at 80°C for 48 h. The hydrochar samples were characterized using BET, FT-IR, and SEM-EDS techniques. Samples produced were labeled HC-200 (Guo et al., 2022).

2.1.4 The Adsorption Procedure for Congo Red

Standard CR solutions (50–100 mg/L) were prepared from a 1000 mg/L stock solution. The maximum wavelength of absorption (503 nm) was determined using a UV-Vis spectrophotometer, and a calibration curve was created. For the adsorption experiments, 0.02 g of adsorbent (cellulose, kaolinite, or activated kaolinite with cellulose) was mixed with 20 mL of a 50 mg/L dye solution and stirred at intervals (0–120 min). Residual dye concentrations were measured using a UV-Vis spectrophotometer, and adsorption parameters were calculated using the Langmuir equation. Thermodynamic studies were conducted by varying dye concentrations (60–100 mg/L) and temperatures (30–60°C).Adsorption capacities, energy, enthalpy, and entropy were determined from the residual concentrations and thermodynamic equations.

2.1.5 Regeneration Adsorbent

The regeneration process was repeated over seven cycles. After each cycle, the adsorbent, which had been desorbed using 20 mL of a selective dye solution at the optimal concentration, was reintroduced. The mixture was stirred for an optimal duration at the ideal temperature, and the remaining dye concentration in the solution was measured using a UV-Vis spectrophotometer.

3. RESULTS AND DISCUSSION

3.1 Characterization of Macroalgae EC and Hydrochar

The FT-IR spectra of EC and its hydrochar produced at 200°C (HC-200) reveal distinct changes in functional groups induced by hydrothermal treatment. Figure 1 shows the FT-IR spectrum of EC macroalgae and the HC-200. A broad peak around 3400 cm^{-1}, representing hydroxyl (O−H) groups, is observed in both EC and HC-200, with slightly reduced intensity in HC-200, suggesting dehydration during the treatment. Figure 1 shows the FT-IR spectrum of materials and BET curve of the materials. Peaks near 2900 cm^{-1}, corresponding to C−H stretching vibrations of aliphatic groups, show reduced intensity in HC-200, likely due

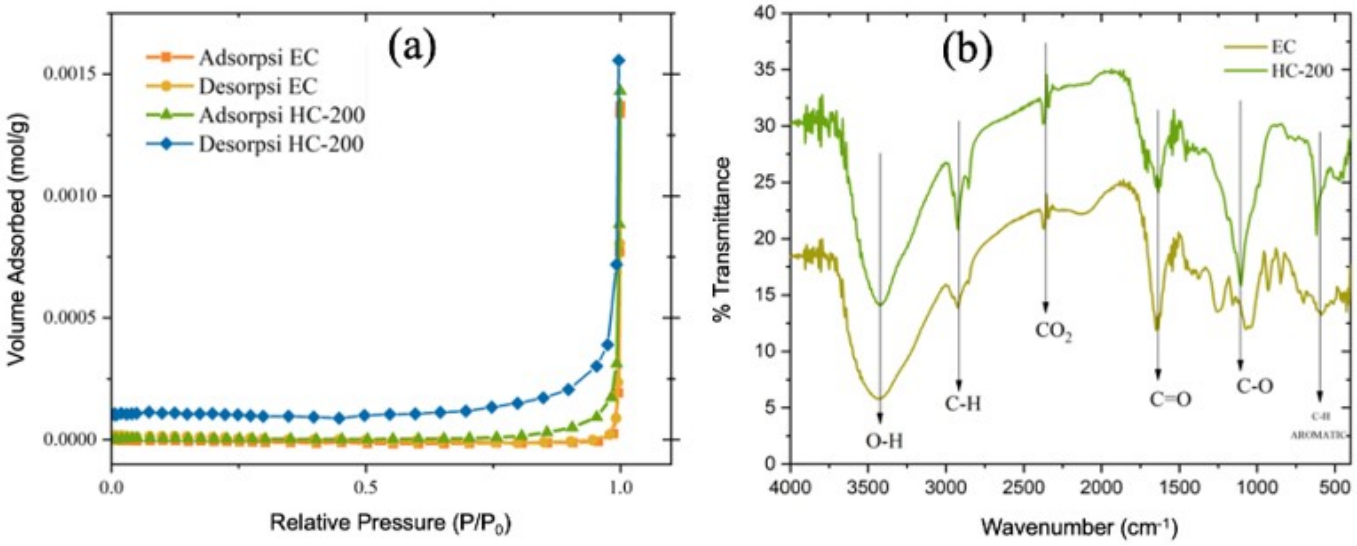

Figure 1. BET Curve of the Materials (a) and Spectrum FT-IR of the Materials (b)

to thermal decomposition. The C=O stretch near 1700 cm^{-1}, associated with carbonyl groups such as carboxylic acids and esters, is diminished in HC-200, indicating reduced oxygenated groups and increased hydrophobicity. Peaks between 1200 and 1000 cm^{-1}, corresponding to C−O stretching of alcohols or esters, and the peak around 800 cm^{-1}, attributed to aromatic C−H bending, highlight structural changes and increased aromaticity in HC-200 (**?**)

BET isotherms for EC and HC-200 exhibit characteristics of type IV or V isotherms, indicative of mesoporosity. The sharp increase in adsorption at high relative pressures (P/P_o) suggests capillary condensation within mesopores. HC-200 shows a significantly higher adsorption capacity compared to EC, reflecting an increase in specific surface area and pore development due to HTC.

Table 1. Surface Area, Average Pore Size and Average Pore Volume of the Materials

Materials	Surface Area (m^2/g)	Average Pore Size (nm)	Average Pore Volume (cm^3/g)
EC	1.5331	136.79	0.04484
HC-200	6.2806	35.177	0.024672

The hysteresis loops in HC-200 further confirm the presence of meso- and macropores, with a more open pore structure compared to EC. Data BET and BJH method in Table 1 indicate that hydrothermal treatment at 200°C enhances the material's surface area and adsorption capacity, making HC-200 more suitable for adsorption applications (Bach et al., 2018).

Figure 2 shows SEM image and the particle distribution curve of the materials. SEM analysis highlights the surface morphology and structural differences between EC and HC-200. EC displays a heterogeneous particle-like structure with rough surfaces and non-uniform size distribution, indicative of high contact areas suitable for adsorption and catalytic applications. Higher magnifications reveal porosity and irregular microstructures, consistent with the polysaccharide-rich composition of EC, which enhances diffusivity for liquids or gases. Table 3. Shows the EDS data of the materials.

Hydrothermal treatment at 200°C induces significant morphological changes in HC-200. At low magnification, HC-200 consists of agglomerated particles with irregular macrostructures, indicative of partial carbonization. At higher magnifications, the surface shows increased roughness and emerging porosity, attributed to the release of volatiles during the process. The presence of spheroids or globules, likely resulting from polymerization and nucleation reactions, signifies structural modification of organic matter.

This morphology aligns with the formation mechanism of hydrochar, where moderate decomposition of lignocellulose and hemicellulose occurs at 200°C. While porosity formation is initiated, further treatment is required to achieve higher surface area and porosity suitable for advanced applications such as catalysis or adsorption (Yu et al., 2022). The average particle distribution for EC is 2100 nm while that for HC-200 is 3550 nm. Visually, the material is uniformly spherical in shape.

The findings from FT-IR, BET, and SEM analyses collectively demonstrate that HTC at 200°C enhances the structural and functional properties of EC, resulting in HC-200 with improved surface area, porosity, and adsorption capacity. These modifications make HC-200 a promising candidate for applications in environmental remediation and material science. The ob-

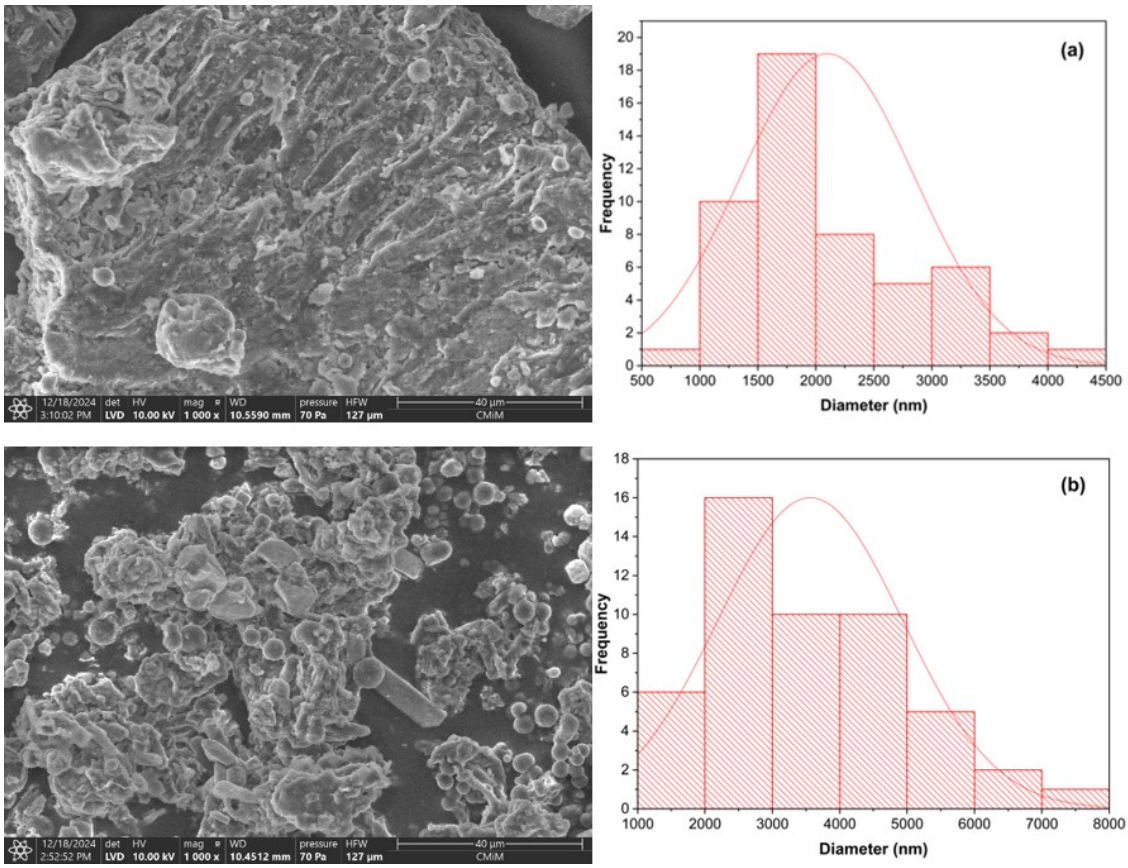

Figure 2. SEM Image and the Particle Distribution Curve of the Materials (a) EC and (b) HC-200

Table 2. The Adsorption Kinetics Data of the Materials

Adsorbent	Qe exp (mg/g)	Pseudo First Order (PFO)			Pseudo Second Order (PSO)		
		Qe calc (mg/g)	k_1 (min^{-1})	R^2	Qe calc (mg/g)	k_2 (g/mg)/min	R^2
EC	25.039	26.82255	0.0256	0.9537	27.5482	0.0014	0.958
HC-200	37.2784	29.5869	0.011515	0.9512	31.6456	0.0013	0.9991

Table 3. EDS Data of the Materials

Materials	%Weight			
	C	O	S	K
EC	51.05	29.02	6.21	6.20
HC-200	64.76	26.74	3.20	3.16

served structural transformations align with previous studies, confirming the potential of algal biomass-derived hydrochars as functional materials (Yu et al., 2021).

3.2 Effect of pHpzc and pH Adsorption

The pH point of zero charge (pHpzc) analysis reveals distinct differences between the raw EC and its hydrochar derivative produced via hydrothermal treatment at 200°C (HC-200). According to Figure 3, the pHpzc of EC is determined to be approximately 6.58, while that of HC-200 is slightly lower, around 6.16. This decrease indicates that the hydrothermal treatment introduces more acidic functional groups, such as carbonyl or carboxyl groups, onto the surface of the material. These changes are likely due to the partial carbonization and the removal of volatile compounds during the hydrothermal process.

The lower pHpzc of HC-200 suggests a more acidic surface compared to EC. At pH values below the pHpzc, the surface of the material becomes positively charged, favoring the adsorption of anionic species such as CR. Conversely, at pH values above the pHpzc, the surface acquires a negative charge, which may repel anions but enhance cation adsorption. The shift in pHpzc from 6.58 to 6.16 for HC-200 implies that this material might exhibit improved adsorption performance for anionic dyes in acidic conditions compared to the untreated EC. In conclusion, hydrothermal treatment at 200°C effectively modifies the surface characteristics of EC, resulting in increased surface acidity and potentially enhanced selectivity for anionic dye adsorption under

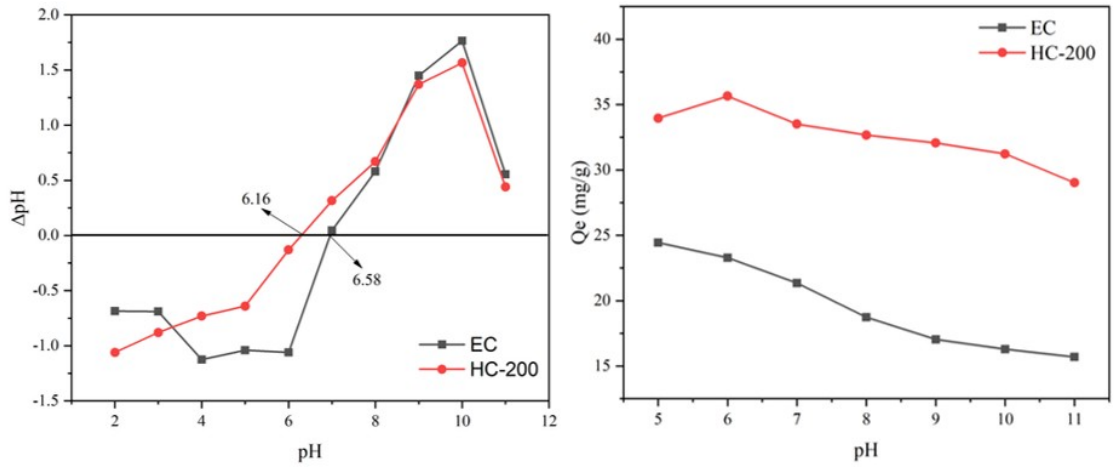

Figure 3. pHpzc Curve and Effect of pH Adsorption Materials

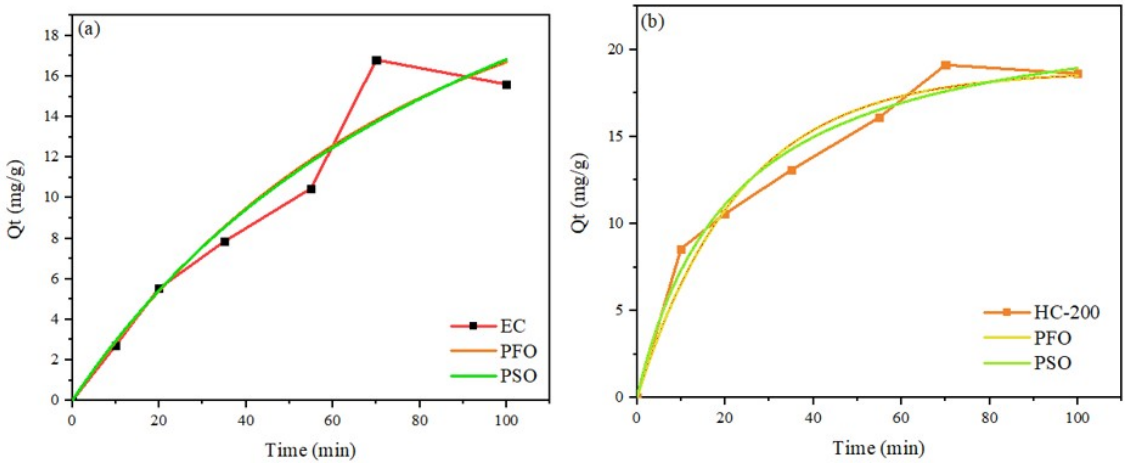

Figure 4. PFO and PSO Curves of the Materials (a) EC and (b) HC

Table 4. Isotherm Adsorption Data of the Materials

Adsorbent	T (°C)	Langmuir			Freundlich		
		Qmax	k_L	R^2	N	k_F	R^2
EC	30	18.99	0.074	0.906	2.653	110.314	0.649
	40	26.035	0.081	0.943	2.968	99.138	0.682
	60	19.546	0.267	0.912	2.809	103.122	0.604
HC-200	30	24.398	0.307	0.914	3.106	95.016	0.656
	40	37.894	0.327	0.943	3.087	95.969	0.687
	50	29.217	0.282	0.926	2.862	102.346	0.627
	60	28.878	0.272	0.92	2.826	102.961	0.626

acidic conditions.

The adsorption results for CR dye onto EC and its hydrochar at 200°C (HC-200) across various pH levels show distinct adsorption behaviors. Generally, HC-200 exhibits higher adsorption capacity (Qe) compared to EC, especially in the acidic to neutral pH range. At pH 6, HC-200 reaches its highest adsorption capacity, around 36 mg/g, indicating favorable adsorption conditions for CR in more acidic environments. As pH increases, the adsorption capacity of HC-200 significantly drops, particularly around pH 9, where it decreases sharply to near-zero. This trend suggests that the electrostatic interactions between the dye molecules and the hydrochar surface are pH-dependent, likely due to changes in surface charge.

Beside, EC reaches its highest adsorption capacity at pH 5,

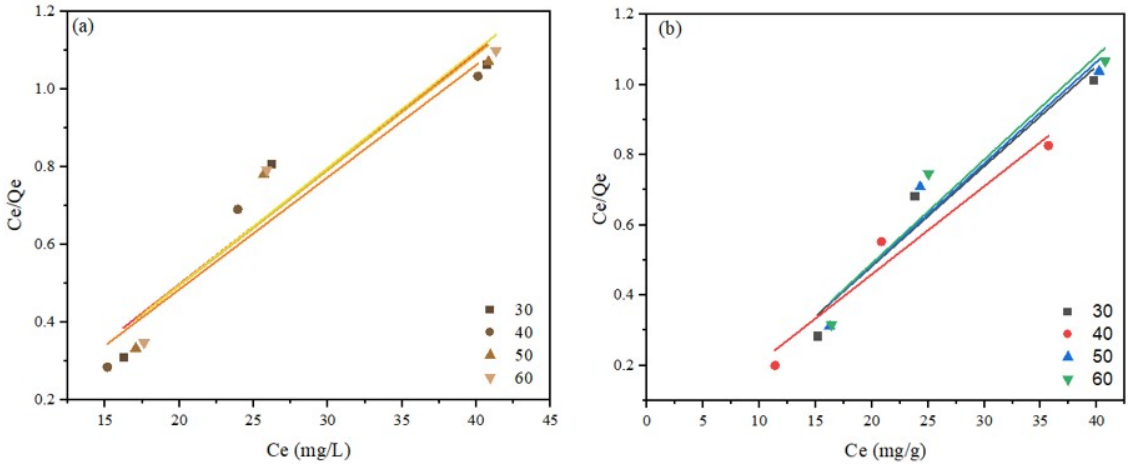

Figure 5. Langmuir Isotherm Curve of the Materials (a) EC and (b) HC-200

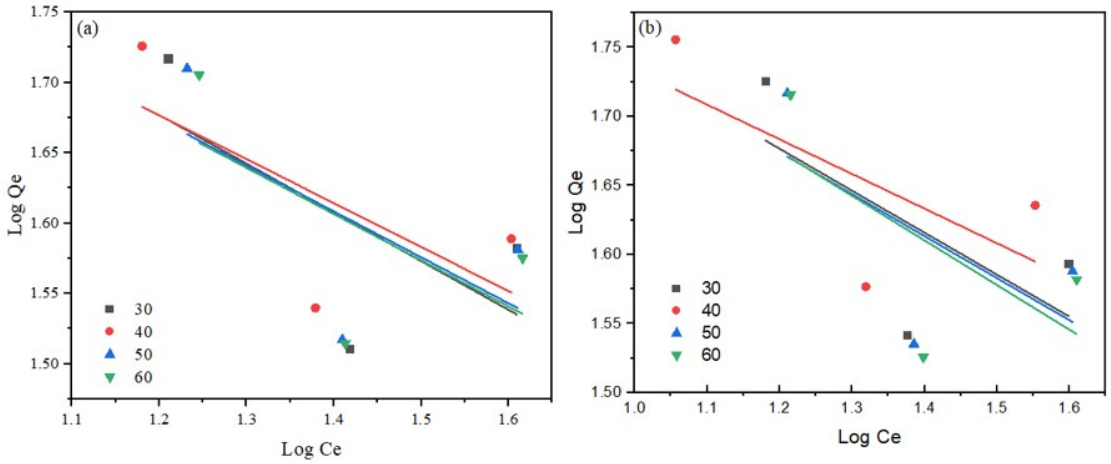

Figure 6. Freundlich Isotherm Curve of the Materials (a) EC and (b) HC-200

around 24 mg/g. The adsorption capacity remains relatively low across all pH levels, peaking only slightly in acidic conditions but showing minimal variation. This indicates that untreated EC has a limited ability to adsorb CR, potentially due to its lower surface area and fewer available active sites compared to the hydrothermally treated HC-200. The sharp decline in adsorption capacity for both materials at higher pH levels could be attributed to the deprotonation of functional groups on the adsorbent surface, which decreases electrostatic attraction toward the anionic dye molecules. Thus, the hydrothermal process appears to enhance the adsorption capacity of EC, with HC-200 showing the best performance at lower pH levels. This analysis highlights the importance of pH in optimizing adsorption processes for dye removal using hydrochar materials, as it significantly influences both the surface charge of the adsorbent and the degree of interaction with anionic dyes like CR.

3.3 Kinetics of Congo Red Adsorption

The adsorption kinetic data for EC and HC-200 reveal distinct adsorption behaviors. The experimental adsorption capacity (Qe exp) shows that HC-200 (37.2784 mg/g) has a significantly higher capacity than EC (25.039 mg/g), likely due to the enhanced surface area and porosity from hydrothermal treatment. When analyzing the data using pseudo-first-order and pseudo-second-order models, it is evident that the pseudo-second-order model provides a better fit for both materials. For EC, the calculated adsorption capacity (Qe calc) in the pseudo-first-order model is 26.82255 mg/g, closely matching the experimental value, with an R^2 of 0.9537. However, for HC-200, the pseudo-first-order model's calculated Qe (29.5869 mg/g) deviates more from the experimental value, with an R^2 of 0.9512, suggesting that this model does not adequately describe the HC-200 adsorption process. Table 2 shows the adsorption kinetics data of the materials.

In contrast, the pseudo-second-order model yields Qe values that align more closely with the experimental data for both materials, especially for HC-200. The calculated Qe for EC

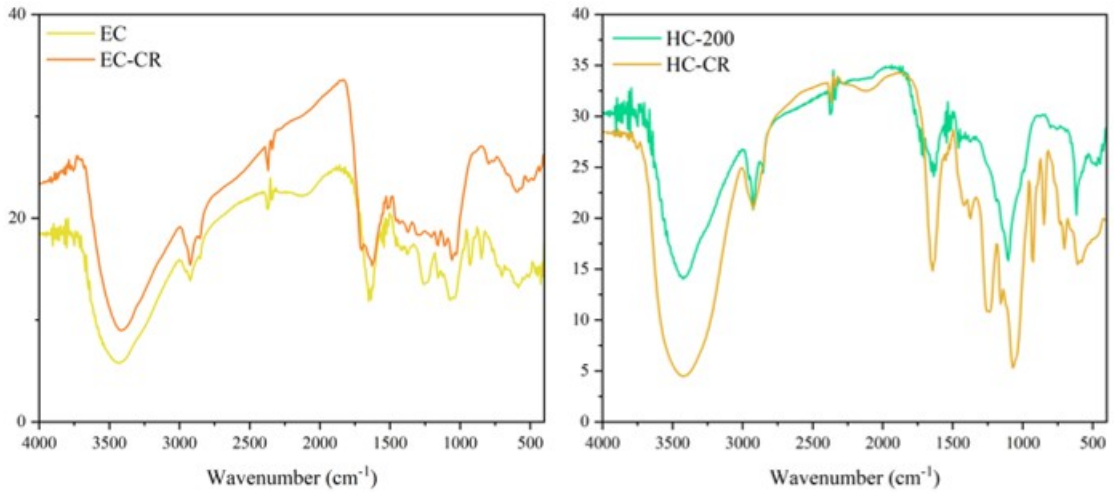

Figure 7. FT-IR Spectrum of the Materials Before and After Adsorption of CR

Table 5. Thermodynamic Data of the Materials.

Adsorbent	Concentration (mg/L)	ΔH (kJ/mol)	ΔS (kJ/mol)	ΔG (kJ/mol)			
				30°C	40°C	50°C	60°C
EC	90	4.021	0.003	3.066	3.034	3.003	2.971
HC-200	90	6.523	0.010	3.528	3.430	3.331	3.232

(27.5482 mg/g) and HC-200 (31.6456 mg/g) under this model shows stronger correlation coefficients (R^2 of 0.958 for EC and 0.9991 for HC-200), suggesting chemisorption as the dominant mechanism, especially for HC-200. Chemisorption, characterized by bond formation between the adsorbate and active sites on the adsorbent, appears to be more prominent in HC-200, contributing to its higher adsorption capacity. Figure 4 shows PFO dan PSO curve of the materials.

Additionally, rate constants show that the pseudo-first-order rate constant (k_1) is higher for EC (0.0256 min^{-1}) than for HC-200 (0.011515 min^{-1}), indicating faster initial adsorption by EC but a lower overall capacity. In the pseudo-second-order model, the rate constants (k_2) for EC and HC-200 are similar (0.0014 and 0.0013 g/mg/min, respectively), but the almost perfect R^2 value for HC-200 further confirms that the pseudo-second-order model best describes the adsorption kinetics. In summary, HC-200 demonstrates higher adsorption capacity and a stronger fit with the pseudo-second-order model, making it a more effective adsorbent for applications that require high adsorption capacity and stronger adsorbate-adsorbent interactions.

3.4 Isotherms Adsorption of Materials

The adsorption isotherm data for EC and HC-200 were analyzed using both the Langmuir and Freundlich models at various temperatures (30°C, 40°C, 50°C, and 60°C) to understand the adsorption characteristics. Figure 5 Shows the Langmuir curve of the materials. According to the Langmuir model, which assumes monolayer adsorption on a homogeneous surface, the maximum adsorption capacity (Qmax) of both materials showed minimal variation with temperature. Table 4 Shows the isotherm adsorption data of the materials.

For EC, Qmax ranged from 19.546 mg/g at 60°C to 26.035 mg/g at 40°C, while HC-200 exhibited a higher Qmax, from 28.878 mg/g at 60°C to 37.894 mg/g at 40°C. This difference in Qmax suggests that HC-200 has a marginally better adsorption capacity than EC, likely due to its enhanced surface area and active sites from hydrothermal treatment. Additionally, the Langmuir constant (k_L) generally increased with temperature for both adsorbents, implying that adsorption affinity improves at higher temperatures, a trend consistent with endothermic adsorption. The Langmuir model correlation coefficients (R^2) were slightly higher for HC-200 (0.92 to 0.943) than for EC (0.906 to 0.943), indicating that HC-200 aligns more closely with monolayer adsorption behavior.

In the Freundlich isotherm analysis, which describes adsorption on heterogeneous surfaces, the Freundlich constant (k_L) values varied with temperature. Figure 6 shows the Freundlich isotherm curve of the materials. For EC, kF ranged from 99.138 to 110.314, while for HC-200, it was slightly lower, between 95.016 and 102.961. These values indicate moderate adsorption intensity, with EC showing slightly higher k_L values, suggesting a somewhat greater adsorption affinity at lower temperatures. The Freundlich exponent (N), which indicates adsorption favorability, remained above 1 for both materials across all temperatures, reflecting favorable adsorption conditions. Notably, HC-200 had N values between 2.826 and 3.106, higher than EC's range of 2.653 to 2.968, suggesting that HC-200 has a more favorable adsorption capacity, especially at lower temperatures. However,

Table 6. Comparison Study of Various Adsorbents Used in the CR Dye Removal from Aqueous Solutions

Material	pH	Qmax (mg/g)	Kinetics Study	Ref
Hydroxyapatite	6.5	40.01	PSO	(Grouli et al., 2024)
Bentonite	6.5	24.74	PSO	(Grouli et al., 2024)
Roots of Eichhornia	-	5.28	PSO	(Wanyonyi et al., 2014)
Tunics of the corm of the saffron	-	6.2	PSO	(Dbik et al., 2020)
Illite Clay	5.7	61.02	PSO	(Altaie et al., 2023)
Cellulose	-	40	PSO	(Tehrani et al., 2024)
Fly ash	-	22.12	PSO	(Harja et al., 2022)
Breadfruit leaf biochar	2	17.8	PSO	(Nguyen et al., 2021)
EC	5	26.035	PSO	This study
Hidrochar from EC	6	37.894	PSO	This study

the R^2 values for the Freundlich model were relatively low (0.604 to 0.687), particularly in comparison to the Langmuir model, indicating that the Freundlich model does not describe the data as well. This suggests that adsorption on both EC and HC-200 is more consistent with monolayer adsorption on a homogeneous surface than with heterogeneous or multilayer adsorption.

Langmuir model provided a better fit for both EC and HC-200, as indicated by higher R^2 values, suggesting monolayer adsorption on relatively homogeneous surfaces. HC-200 demonstrated slightly better adsorption capacity and affinity than EC, likely due to structural improvements from hydrothermal treatment. The increasing k_L values with temperature indicate that adsorption is endothermic, and HC-200's enhanced adsorption properties make it a more effective adsorbent, particularly at moderately elevated temperatures.

3.5 Thermodynamics Adsorption of Materials

The thermodynamic analysis reveals distinct adsorption characteristics of CR dye on two types of adsorbents: HC-200 and EC. Table 5 shows thermodynamic data of the materials. The enthalpy change (ΔH) for both adsorbents is mostly positive, indicating that the adsorption process is endothermic and requires heat absorption. HC-200 exhibits higher ΔH values than EC at the same concentrations, suggesting a stronger endothermic interaction, potentially due to a larger number of binding sites or a higher affinity for CR.

The entropy change (Δs) for both adsorbents is generally small and positive, indicating an increase in disorder at the solid-liquid interface during adsorption. HC-200 tends to have higher Δg values than EC, suggesting that HC-200 induces a greater degree of structural disorder upon adsorption. Furthermore, the Gibbs free energy change (ΔG) varies with temperature and concentration. Negative ΔG values at certain concentrations, such as for EC at 60 mg/L and 100 mg/L, and for HC-200 at 60 mg/L, indicate that the adsorption process is spontaneous under these conditions. However, at higher concentrations, ΔG values are often positive, implying that the adsorption process is less spontaneous at those conditions.

Overall, HC-200 shows higher ΔH and ΔS values, as well as a broader range of negative ΔG values, indicating that HC-200 is more effective in adsorbing CR across a range of temperatures and concentrations compared to EC. This suggests that HC-200 may have a higher adsorption capacity, possibly due to a larger surface area or different surface characteristics resulting from the pyrolysis process at 200°C. The endothermic nature of the adsorption process for both adsorbents indicates that higher temperatures can enhance adsorption efficiency. In summary, this thermodynamic study highlights HC-200 as a more promising adsorbent for CR, especially at elevated temperatures, whereas EC exhibits limited adsorption potential at higher concentrations.

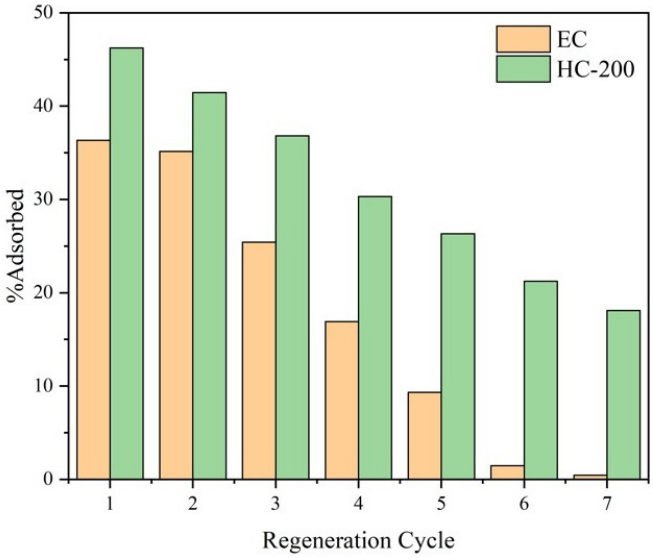

Figure 8. Regeneration Cycles of the Materials

3.6 Post-Adsorption FT-IR Characterization of EC and HC Materials

Macroalgae and hydrochar materials that have absorbed CR are then subjected to a drying process, followed by re-characterizati on using FT-IR. This procedure allows for the observation of changes in the material's structure due to the absorption of CR. Figure 7 shows the comparison of the FT-IR spectrum of the material before and after adsorption.

The FT-IR spectra demonstrated that following the absorption of CR, there was a substantial decrease in the absorption intensity of the functional groups on the EC, as evidenced by the decline in %Transmittance (%T). This observation suggests the involvement of polar functional groups of the EC in the chemical adsorption process. In contrast, the HC exhibited an increase in %T after CR adsorption. This phenomenon can be explained by the "closing" effect on the pores of HC, where significant amounts of adsorbed CR molecules cover the active surface of HC, reducing the exposure of HC functional groups to IR radiation.

3.7 Regeneration Study of Materials

The regeneration performance of EC and its hydrochar derivative produced via hydrothermal treatment at 200°C (HC-200) was evaluated over seven regeneration cycles. The results, expressed as the percentage of adsorbed material, demonstrate distinct differences in the stability and reusability of these adsorbents.

Figure 8 shows the regeneration cycles of the materials. In the first cycle, HC-200 exhibits a higher adsorption percentage (~ 47%) compared to EC (~ 35%), highlighting its superior initial performance. As the regeneration cycles progress, a notable decline in adsorption capacity is observed for both materials. However, HC-200 consistently outperforms EC across all cycles. By the third cycle, HC-200 retains a significant adsorption capacity (~ 40%), while EC drops below ~ 20%. The trend continues with HC-200 maintaining a measurable adsorption efficiency even at the seventh cycle (~ 25%), whereas EC shows minimal or negligible adsorption capability beyond the fifth cycle. These findings suggest that the hydrothermal treatment at 200°C not only enhances the initial adsorption performance of EC but also improves its structural stability and resilience during multiple regeneration cycles. The higher durability of HC-200 is likely due to its modified surface properties and reduced loss of active sites during regeneration. In addition, HC-200 demonstrates higher adsorption capacity compared to untreated EC and several adsorbents (Table 6), making it a more sustainable and cost-effective adsorbent for repeated use in dye removal applications. This highlights the potential of hydrothermal modification in enhancing the operational lifespan of biomass-based adsorbents.

4. CONCLUSIONS

This study highlights the significant enhancements achieved in EC (EC) through hydrothermal carbonization at 200°C, yielding hydrochar (HC-200) with improved adsorption properties. Adsorption studies demonstrate HC-200's superior performance, with pHpzc analysis indicating more acidic surface characteristics that enhance selectivity for anionic dyes under acidic conditions. Kinetics align best with the pseudo-second-order model, and thermodynamic analysis shows an endothermic and spontaneous adsorption process, particularly efficient at higher temperatures. Furthermore, HC-200 exhibits excellent stability and reusability, retaining substantial adsorption efficiency over seven regeneration cycles, unlike EC, which shows diminished performance with repeated use. The comprehensive findings from FT-IR, BET, SEM, adsorption, and thermodynamic analyses underscore HC-200's enhanced properties. In conclusion, hydrothermal carbonization at 200°C transforms EC into a highly effective material for environmental remediation and dye adsorption. Future research should optimize carbonization conditions and explore functionalization techniques to expand its industrial and environmental applications.

5. ACKNOWLEDGEMENT

Thanks to Hibah Profesi Universitas Sriwijaya No. 0016/UN9/SK. LP2M.PT/2024 for the financial support in this research. Also, the Research Center of Inorganic Materials and Coordination Complexes at Sriwijaya University provided support and analytical assistance that enabled the author to complete this inquiry.

REFERENCES

Altaie, O. T. S., H. S. Jassim, and G. M. Hadi (2023). Removal of Congo Red from Aqueous Solutions by Adsorption onto Illite Clay. *Desalination and Water Treatment*, **310**; 226–237

Bach, L. G., T. Van Tran, T. D. Nguyen, T. Van Pham, and S. T. Do (2018). Enhanced Adsorption of Methylene Blue onto Graphene Oxide-Doped XFe_2O_4 (X = Co, Mn, Ni) Nanocomposites: Kinetic, Isothermal, Thermodynamic and Recyclability Studies. *Research on Chemical Intermediates*, **44**(3); 1661–1687

Blondeau, J. and H. Jeanmart (2012). Biomass Pyrolysis at High Temperatures: Prediction of Gaseous Species Yields from an Anisotropic Particle. *Biomass and Bioenergy*, **41**; 107–121

Bridgwater, A. V. (2012). Review of Fast Pyrolysis of Biomass and Product Upgrading. *Biomass and Bioenergy*, **38**; 68–94

Chen, N., S. Cao, L. Zhang, X. Peng, X. Wang, Z. Ai, and L. Zhang (2021). Structural Dependent Cr (VI) Adsorption and Reduction of Biochar: Hydrochar Versus Pyrochar. *Science of the Total Environment*, **783**; 147084

Dbik, A., A. Dbik, M. Chaouch, N. E. Messaoudi, A. Lahkimi, F. Bentahar, and M. Chiban (2020). Adsorption of Congo Red Dye from Aqueous Solutions Using Tunics of the Corm of the Saffron. *Materials Today: Proceedings*, **22**; 134–139

de Tuesta, J. L. D., M. C. Saviotti, F. F. Roman, G. F. Pantuzza, H. J. Sartori, A. Shinibekova, M. S. Kalmakhanova, B. K. Massalimova, J. M. Pietrobelli, and G. G. Lenzi (2021). Assisted Hydrothermal Carbonization of Agroindustrial Byproducts as Effective Step in the Production of Activated Carbon Catalysts for Wet Peroxide Oxidation of Micro-Pollutants. *Journal of Environmental Chemical Engineering*, **9**(1); 105004

Deng, X., Y. Liu, L. Wang, Q. Chen, X. Guo, C. Xu, Y. Zhang, Y. Shi, and W. Shen (2024). Composite Adsorbents of Aminated Chitosan @ZIF-8 MOF for Simultaneous Efficient Removal of Cu(II) and Congo Red: Batch Experiments and DFT Calculations. *Chemical Engineering Journal*, **479**; 147634

El Bourachdi, S., F. Moussaoui, A. R. Ayub, A. El Amri, F. El Ouadrhiri, A. Adachi, A. Bendaoud, A. M. Idrissi, and A. Lahkimi (2025). DFT Theoretical Analysis, Experimental Approach, and RSM Process to Understand the Congo Red

Adsorption Mechanism on Chitosan@Graphene Oxide Beads. *Journal of Molecular Structure*, **1321**; 140090

Farobie, O., A. Amrullah, L. A. Anis, E. Hartulistiyoso, N. Syaftika, G. Saefurahman, and A. Bayu (2023). Valorization of Brown Macroalgae *Sargassum plagiophyllum* for Biogas Production under Different Salinity Conditions. *Bioresource Technology Reports*, **22**; 101403

Funke, A. and F. Ziegler (2010). Hydrothermal Carbonization of Biomass: A Summary and Discussion of Chemical Mechanisms for Process Engineering. *Biofuels, Bioproducts and Biorefining*, **4**(2); 160–177

Ghosh, S., A. Biswas, S. Saha, S. Jana, P. Roy, D. Paul, and A. Ghosh (2021). Elucidation of Selective Adsorption Study of Congo Red Using New Cadmium(II) Metal-Organic Frameworks: Adsorption Kinetics, Isotherm and Thermodynamics. *Journal of Solid State Chemistry*, **296**; 121929

Grouli, A., N. El Messaoudi, A. Dbik, M. El Messaoudi, M. Chiban, and F. Bentahar (2024). An Investigation of the Adsorption of Congo Red Dye on Two Naturally Occurring Adsorbents Hydroxyapatite and Bentonite: An Experimental Analysis, DFT Calculations, and Monte Carlo Simulation. *Heliyon*, **10**(21); e39884

Guo, J., F. Shi, M. Sun, F. Ma, and Y. Li (2022). Antioxidant and Aflatoxin B1 Adsorption Properties of *Eucheuma cottonii* Insoluble Dietary Fiber. *Food Bioscience*, **50**; 102043

Harja, M., G. Buema, and D. Bucur (2022). Recent Advances in Removal of Congo Red Dye by Adsorption Using an Industrial Waste. *Scientific Reports*, **12**(1); 1–18

Hoekman, S. K., A. Broch, and C. Robbins (2011). Hydrothermal Carbonization (HTC) of Lignocellulosic Biomass. *Energy and Fuels*, **25**(4); 1802–1810

Kruse, A. and N. Dahmen (2018). Hydrothermal Biomass Conversion: Quo Vadis. *Journal of Supercritical Fluids*, **134**(December 2017); 114–123

Kumar, M., A. O. Oyedun, and A. Kumar (2018). A Review on the Current Status of Various Hydrothermal Technologies on Biomass Feedstock. *Renewable and Sustainable Energy Reviews*, **81**(March 2017); 1742–1770

Lesbani, A., N. Ahmad, S. Wibiyan, A. Wijaya, Y. Hanifah, I. Royani, R. Mohadi, et al. (2025). Improving Congo Red Dye Removal by Modification Layered Double Hydroxide with Microalgae and Macroalgae: Characterization and Parametric Optimation. *Colloids and Surfaces A: Physicochemical and Engineering Aspects*, **706**; 135770

Munir, M. T., S. S. Mansouri, I. A. Udugama, S. Baroutian, K. V. Gernaey, and B. R. Young (2018). Resource Recovery from Organic Solid Waste Using Hydrothermal Processing: Opportunities and Challenges. *Renewable and Sustainable Energy Reviews*, **96**; 64–75

Nguyen, D. L. T., Q. A. Binh, X. C. Nguyen, T. T. H. Nguyen, Q. N. Vo, T. D. Nguyen, T. C. P. Tran, T. A. H. Nguyen, S. Y. Kim, T. P. Nguyen, J. Bae, I. T. Kim, and L. Q. Van (2021). Metal Salt-Modified Biochars Derived from Agro-Waste for Effective Congo Red Dye Removal. *Environmental Research*, **200**(March); 111492

Ramesh, N., C. W. Lai, M. R. B. Johan, S. M. Mousavi, I. A. Badruddin, A. Kumar, G. Sharma, and F. Gapsari (2024). Progress in Photocatalytic Degradation of Industrial Organic Dye by Utilising the Silver Doped Titanium Dioxide Nanocomposite. *Heliyon*, **10**(December 2024); e40998

Tehrani, A. D., F. Tahriri, A. K. Najafabadi, and K. Arefizadeh (2024). Preparation of New Green Poly (Amino Amide) Based on Cellulose Nanoparticles for Adsorption of Congo Red and Its Adaptive Neuro-Fuzzy Modeling. *International Journal of Biological Macromolecules*, **281**(P1); 136287

Wanyonyi, W. C., J. M. Onyari, and P. M. Shiundu (2014). Adsorption of Congo Red Dye from Aqueous Solutions Using Roots of Eichhornia Crassipes: Kinetic and Equilibrium Studies. *Energy Procedia*, **50**; 862–869

Wibiyan, S., A. Wijaya, and P. M. S. B. N. Siregar (2023). Adsorption of Phenol Using Cellulose and Hydrochar: Kinetic, Isotherm, and Regeneration Studies. *Indonesian Journal of Material Research*, **1**(2); 61–67

Yu, J., T. Tang, F. Cheng, D. Huang, J. L. Martin, C. E. Brewer, R. L. Grimm, M. Zhou, and H. Luo (2021). Exploring Spent Biomass-Derived Adsorbents as Anodes for Lithium Ion Batteries. *Materials Today Energy*, **19**

Yu, S., X. Yang, P. Zhao, Q. Li, H. Zhou, and Y. Zhang (2022). From Biomass to Hydrochar: Evolution on Elemental Composition, Morphology, and Chemical Structure. *Journal of the Energy Institute*, **101**(December 2021); 194–200

